Tetrahedron 75 (2019) 518–526

Contents lists available at ScienceDirect

Tetrahedron

journal homepage: www.elsevier.com/locate/tet

Switchable pyrrole-based hydrogen bonding motif in enantioselective trifunctional organocatalysis

Sviatoslav S. Eliseenko, Fei Liu *, *

Department of Molecular Sciences, Macquarie University, Sydney, NSW 2109, Australia

ARTICLE INFO

Article history:
Received 11 October 2018
Received in revised form
10 December 2018
Accepted 11 December 2018
Available online 19 December 2018

Keywords:
Switchable catalysis
Cooperativity
Trifunctional organocatalysis
Enantioselectivity
Pyrroles
Morita–Baylis–Hillman reaction

ABSTRACT

Pyrroles are versatile chemical motifs for molecular recognition or ligand design but their utility as catalytic components are underexplored. We incorporated a pyrrole motif into our acid-switchable, MAP-based trifunctional organocatalytic system. The switching-on of this system by an external Brønsted acid, 3-methyl benzoic acid, presented proficient catalysis in both *aza*-Morita–Baylis–Hillman (MBH, up to >95% conversion and 88% *ee* over 3 h) and MBH (up to 81% conversion and 77% *ee* over 6 h) reactions. The enhanced catalytic generality and proficiency may be due to the new cooperativity via CH/π interactions between pyrrole and the acid switch.

© 2018 Elsevier Ltd. All rights reserved.

1. Introduction

Pyrroles are chemical motifs prevalent in bioactive compounds [1], ligands [2], sensors [3], and molecular assemblies [4]. The versatile chemistry of pyrroles in part derives from the multifunctional pyrrolyl NH group that is weakly acidic and basic, in addition to the electron-rich π system primed for electrophilic substitution reactions and also hydrogen-bonding interactions [5]. The role of pyrroles as catalytic components, however were mainly explored within the context of calix[4]pyrrole systems and remain under developed [6]. More recently, pyrrole NH motifs have been used in hydrogen bonding catalysis as part of a tunable H-bonding catalyst [6a,c], expanding significantly from its normal coordination role as a ligand. Questions now can be raised on new roles of pyrrole in switchable catalysis [7] given pyrrole's multifunctional nature. Here we report a novel example of a pyrrole-containing, acid-switchable, enantioselective trifunctional organocatalytic system with enhanced generality and enantioselectivity, likely due to the multifunctional aspect of the pyrrole motif involving not only the NH hydrogen-bond donor but also the π electron system through CH/π hydrogen bonding [8]. This catalysis extends beyond the typical role of pyrrole as a coordination or pH switching site.

We have, in our prior work, originated a switchable, enantioselective trifunctional organocatalytic prototype for activating enones in carbon-carbon bond forming reactions such as the Morita–Baylis–Hillman (MBH) reaction (Fig. 1a) [9]. The prototype trifunctional system is built on a very versatile MAP-based chemical system [10]. The MAP-based catalysts typically contain three catalytic motifs: a phosphine nucleophile for reaction initiation, an amine Brønsted base for responding to the external acid switch, and a phenol Brønsted acid for H-bonding interactions that help stabilize the formation of zwitterionic intermediates [9,11]. An external, strong Brønsted acid additive, such as benzoic acid, switches the catalysis from slow and racemic to fast and enantioselective, particularly for the *aza*-MBH reactions that are often slow in rate with capricious catalytic scope [12]. We have also investigated multiple generations of this system by tuning the acidity of the internal Brønsted acid motif [12f,13a,11,13b,c,9], and in all cases, benzoic acid has been the best additive to switch on the fast and enantioselective catalysis. One persistent issue for this switchable system however is to extend the generality to cover not just the *aza*-MBH but also the MBH reactions. One potential solution is to find more synergistic noncovalent interactions between the acid-activator and the catalyst. This may also address a long-standing challenge of engineering compact molecular assemblies with tunable catalytic properties that require a more synergistic

* Corresponding author.
E-mail address: fei.liu@mq.edu.au (F. Liu).

https://doi.org/10.1016/j.tet.2018.12.016
0040-4020/© 2018 Elsevier Ltd. All rights reserved.

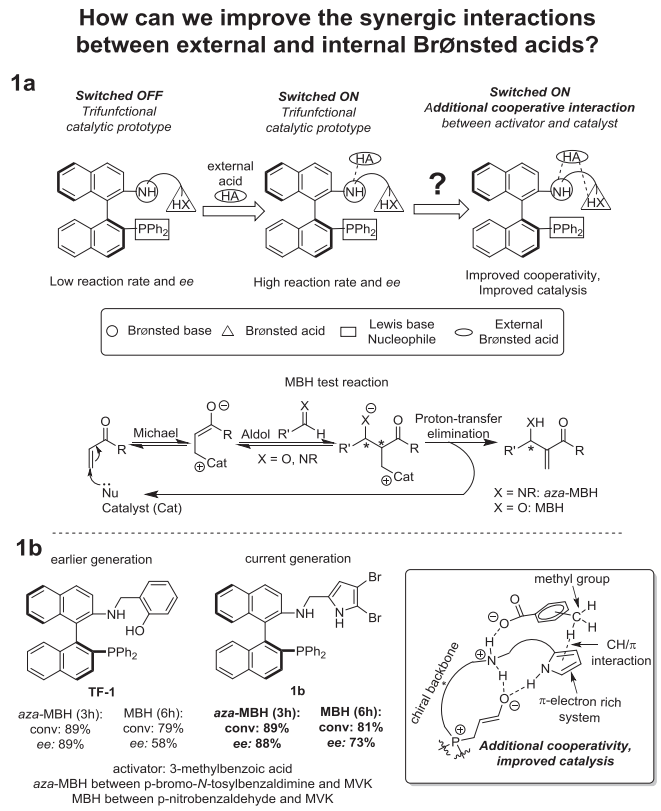

Fig. 1. a) Switchable and enantioselective trifunctional organocatalytic prototype given a general mechanism of a test MBH reaction; **b)** Enhancing switchable catalysis with multifunctional recognition motifs such as pyrroles.

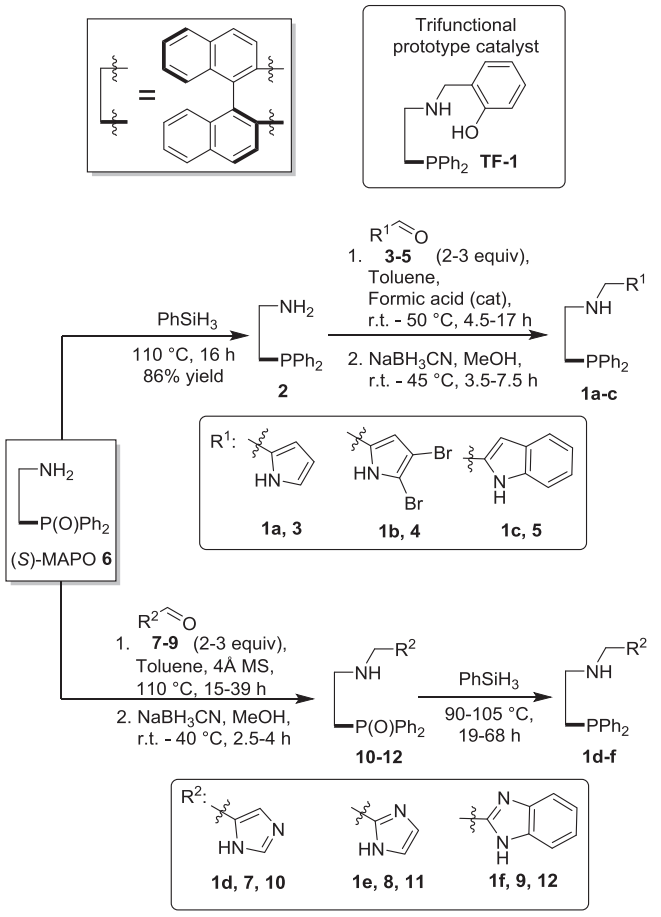

Scheme 1. Synthesis of catalysts **1a**–**f**.

network of molecular recognition arrangements.

To test this hypothesis, we investigated the potential of the multifunctional pyrrole motif that contains weakly acidic NH group for H-bonding interactions and the electron-rich π system that could act, in close spatial proximity, as an H bond acceptor that may enhance the interaction with the external acid activator (Fig. 1b). We found that a pyrrole-based catalyst, activated by 3-methyl benzoic acid, provided catalytic improvement in MBH catalysis with an increase in *ee* by 15% (approx. 1.5 fold by *e.r.*, up to 73%), in comparison to our earlier generations of catalysts such as trifunctional catalyst **TF-1**. Pyrrole phosphines were previously used as *N*-phosphinepyrrole ligands in complexes with Rh in hydroformylations [14], Pd in CO-ethene co-polymerization [15], Pt in benzene vinylation [16], and Ir in enantioselective hydrogenation [17]. The complexation patterns of *N*-pyrrole-phosphine ligands with Cr, Ru, Mo, W, and Se were also reported [18]. The 2-phosphino-*N*-aryl or alkyl substituted pyrroles were investigated as ligands for Pd [19] and Ru [20]. The ligands where both pyrrole and phosphine fragments bind Ni [21] or Cu [22] were also described. Pyrrole-containing phosphines are also known as bioactive molecules [23]. However, phosphine pyrroles have not been used previously as organocatalysts and our chiral phosphine–pyrrole system here represents the first set of such examples.

2. Results and discussion

A series of pyrrole-containing catalysts were designed and synthesized (Scheme 1). The unsubstituted pyrrole catalyst **1a** was synthesized as the base model, and other catalysts, **1b**–**f**, were developed to vary the acidity of the pyrrole NH motif and its steric factor. Considering that changing the Brønsted acid motif acidity can improve the catalytic proficiency [13c], catalysts **1d**–**f** containing more acidic imidazole motifs were also investigated for comparison. The additional steric variation may influence the enantioselectivity by biasing the substrate approach. To investigate the steric influence around the pyrrolic NH center, catalysts **1b**, **c**, **f** containing sterically bulky and electron withdrawing bromine atoms or fused benzene ring were synthesized. Catalysts **1c** and **1f** contain benzimidazolyl and benzopyrrolyl fragments with a more extended π system that may also influence the catalytic proficiency via π interactions with the substrate or external acid activator. Tuning of the phosphine Lewis base was not attempted, as our prior investigations (unpublished data) indicated that adding substituents onto the aryl phosphine to increase the Lewis base nucleophilicity actually resulted in loss of catalysis, likely due to unexpected interference with the acid switch.

The synthesis of new catalysts **1a**–**f** was performed by modified reported procedures [9] from the key intermediate (*S*)-MAPO **6** [10a-c,24,9] in 2 steps (Scheme 1). For the synthesis of pyrrolyl- and indolyl-containing catalysts **1a**–**c,** the aminophosphine **2** was initially synthesized from **6** by chemoselective phosphine oxide reduction. Further reductive amination of the corresponding aldehydes **3**–**5** by aminophosphine **2** furnished catalysts **1a**–**c** (Scheme 1). Attempts to synthesize imidazolyl- and benzimidazolyl-containing catalysts **1d**–**f** were met with significant difficulties as phosphine oxidation occurred during the reductive amination step. Therefore, the reductive amination of aldehydes **7**–**9** was performed with (*S*)-MAPO **6**, followed by a subsequent phosphine oxide reduction to afford catalysts **1d**–**f**

(Scheme 1).

The synthesis of **11** and **1e** required up to 70 h of reactions whereas all other catalysts and their phosphine oxide precursors can be synthesized in much less time (~20 h). The purification of catalysts **1a**–**f** and precursors **10**–**12** were challenging due to the low stability of these compounds [25]. Catalyst **1b** was chosen for solvent screening due to its easier purification process (Table 1). Consistent with earlier hallmark profiles of our trifunctional organocatalysts, dichloromethane and diethyl ether were the best solvents for the *aza*-MBH and MBH model reactions, respectively (Table 1, entries 1 and 10) [11,13c,9]. More polar solvents such as acetonitrile resulted in poor yields and low enantioselectivity (Table 1, entries 6 and 13). No product formation occurred in polar protic solvents such as methanol (Table 1, entries 7 and 14). This confirms our working hypothesis that this enantioselective trifunctional catalysis relies on ion pairing upon activation by an acid additive.

After the identification of the best solvent for the *aza*-MBH and MBH test reactions, the external acid additives were screened (Table 2). For comparison, model **TF-1** (Scheme 1) was also tested (Table 2, entries 24, 25). The response of switching on catalytic proficiency (coupled rate and *ee* enhancement) to the acid activation is one of the main criteria of a trifunctional catalysis mode [9], in which the activation by an external acid likely occurs via the participation of its counterion in the irreversible, final proton-transfer step [9,11]. Benzoic acid (pK_a 4.20) was found to be the best activator for previous generations of catalysts [11,13c,9]. Therefore, a set of aromatic acids with comparable pK_a values was tested along with other types of organic acids such as phenylphosphinic and acetic acids (Table 2). Interestingly, 3-methyl benzoic acid (pK_a 4.24) was found to be the best acid additive for both the *aza*-MBH and MBH test reactions, providing the corresponding products in the good *ee* (88% for *aza*-MBH; 73% for MBH) and good yields (Table 2, entries 6 and 13). Notably, benzoic acid, which was the best activator for previous generations of catalysts, demonstrated lower proficiency than 3-methyl benzoic acid, providing *aza*-MBH and MBH products in 84% and 70% *ee*, respectively (Table 2, entries 1 and 11). The 3-chloro- and 4-cyanobenzoic acid additive with lower pK_a values (3.83 and 3.55 correspondingly) provided significant rate loss in the MBH reaction (Table 2, entries 15, 16), suggesting likely quenching of the zwitterionic intermediate via protonation [12d].

Benzoic acid and 3-methyl benzoic acid both have comparable pK_a values, but 3-methyl benzoic acid provided better results with little observable steric interference. A further test of 2-methylbenzoic acid with a significantly lower pK_a than 3-methylbenzoic acid (3.91 vs. 4.24 correspondingly) demonstrated a comparable proficiency in both *aza*-MBH and MBH reactions (Table 2, entries 6 and 13 vs. 7 and 14). These results suggest an important role of the methyl substituent in the acid additive for the proficient catalysis that is independent of the pK_a. Such an improvement with a bulkier acid activator is unexpected and may be explained by the additional CH/π hydrogen bonding stabilization possibly between the electron rich pyrrole fragment of the catalyst and methyl group of the external acid additive (Scheme 1b).

The screening of the acid additive influence on the imidazolyl-containing catalyst **1d** provided a comparable trend albeit at

Table 1
Solvent screening of **1b**-catalyzed *aza*-MBH and MBH reactions.

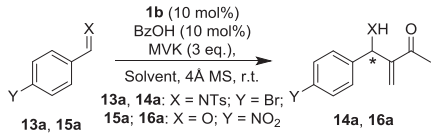

Entry	X (Y)	Solvent	Time [h]	Conv[a] (*ee*[b]) [%]
1	NTs (Br)	DCM	3	77 (84)
2	NTs (Br)	Chloroform	3	73 (79)
3	NTs (Br)	Ether	3	95[c] (59)
4	NTs (Br)	THF	3	89 (76)
5	NTs (Br)	Toluene	3	>95[c] (73)
6	NTs (Br)	Acetonitrile	3	50[c] (18)
7	NTs (Br)	Methanol	24	No reaction (n.d.)
8	O (NO_2)	DCM	6	17 (69)
9	O (NO_2)	Chloroform	6	18 (64)
10	O (NO_2)	Ether	6	75 (70)
11	O (NO_2)	THF	6	29 (69)
12	O (NO_2)	Toluene	6	53 (73)
13	O (NO_2)	Acetonitrile	6	8 (39)
14	O (NO_2)	Methanol	24	No reaction (n.d.)

[a] Calculated by ^{1}H NMR spectroscopy.
[b] Determined by chiral HPLC analysis.
[c] 27 mol% loading of **1b**.

Table 2
Acid additive and loading screening of *aza*-MBH and MBH reactions.

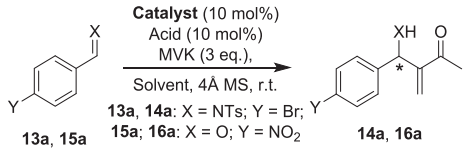

Entry	Catalyst	X (Y)	Acid additive	Solvent	Time [h]	Conv[a] (*ee*[b]) [%]
1	**1b**	NTs (Br)	BzOH	DCM	3	77 (84)
2	**1b**	NTs (Br)	4-F-BzOH	DCM	3	62 (85)
3	**1b**	NTs (Br)	2-Naphthoic	DCM	3	60 (81)
4	**1b**	NTs (Br)	Acetic	DCM	3	>95 (80)
5	**1b**	NTs (Br)	Phenylphosphinic	DCM	24	8 (−2)
6	**1b**	NTs (Br)	**3-Me-BzOH**	**DCM**	**3**	**89 (88)**
7	**1b**	NTs (Br)	2-Me-BzOH	DCM	3	>95 (86)
8	**1d**	NTs (Br)	BzOH	DCM	3	29 (*56*)
9	**1d**	NTs (Br)	4-F-BzOH	DCM	3	25 (*54*)
10	**1d**	NTs (Br)	3-Me-BzOH	DCM	3	27 (*60*)
11	**1b**	O (NO_2)	BzOH	Ether	6	75 (70)
12	**1b**	O (NO_2)	4-F-BzOH	Ether	6	70 (69)
13	**1b**	O (NO_2)	**3-Me-BzOH**	**Ether**	**6**	**81 (73)**
14	**1b**	O (NO_2)	2-Me-BzOH	Ether	6	85 (74)
15	**1b**	O (NO_2)	3-Cl-BzOH	Ether	6	11 (69)[c]
16	**1b**	O (NO_2)	4-CN-BzOH	Ether	6	>5 (61)[c]
17	**1b**	O (NO_2)	Acetic	Ether	6	81 (51)
18	**1b**	O (NO_2)	Phenylphosphinic	Ether	24	7 (34)
19	**1b**	O (NO_2)	1-Naphthoic	Ether	6	35 (69)
20	**1b**	O (NO_2)	2-Naphthoic	Ether	6	62 (73)
21	**1d**	O (NO_2)	BzOH	Ether	24	70 (*39*)
22	**1d**	O (NO_2)	3-Me-BzOH	Ether	24	93 (*39*)
23	**1d**	O (NO_2)	2-Naphthoic	Ether	24	70 (*37*)
24	**TF-1**	NTs (Br)	3-Me-BzOH	DCM	3	89 (*89*)
25	**TF-1**	O (NO_2)	3-Me-BzOH	Ether	6	79 (*58*)

[a] Calculated by ^{1}H NMR spectroscopy.
[b] Determined by chiral HPLC analysis.
[c] *ee* level determined for conversion after 24 h.

lower proficiency (Table 2, entries 8–10 and 21–23). We have shown [13c] that the acidity and the spatial position of the Brønsted acid motif on the catalyst will impact on the proficiency of the catalysis. The lower proficiency (e.g. slower rate and lower enantioselectivity) of the imidazole-containing catalysts, compare to the pyrrole series, may be due to the higher acidity of the imidazole NH and also the position of the NH proton. The activity of **1b**, activated by 3-methyl benzoic acid, is comparable to the control, phenol-containing catalyst **TF-1** in the test *aza*-MBH reaction, but noticeably higher in the MBH reaction (Table 2, entries 1, 11 vs 24, 25). Thus, catalyst **1b** provided the highest enantioselectivity in MBH test reactions among other generations of MAP-base trifunctional catalysts, likely due to the aforementioned additional CH/π cooperation in the switchable catalytic system [11,13c,9].

For catalyst **1b**, the acid additive loading effect was next investigated and found to be consistent for both *aza*-MBH and MBH reactions (Table 3). The use of an acid loading more than the equimolar loading to catalyst **1b** showed significant erosion of both reaction rate and enantioselectivity in the *aza*-MBH reaction (Table 3, entries 5, 6 vs 4), but only erosion of the reaction rate in the MBH test reaction (Table 3, entries 14, 13 vs 12). Less than equimolar acid additive loading to that of the catalyst demonstrated slight reduction in proficiency for *aza*-MBH test reactions (Table 3, entry 3 vs 4) and slightly higher reaction rates in MBH test reactions albeit in lower enantioselectivity (Table 3, entry 11 vs 12). The catalytic profile of the pyrrole catalysts is different from that of phenol-containing catalyst **TF-1** as this catalyst demonstrated the highest proficiency at 5 equivalent loading of an acid additive to the catalyst [9]. The catalyst loading, as expected, influenced mostly the reaction rate, providing a higher rate at a higher loading (Table 3). The enantioselectivity of test reactions did not vary as significantly with different catalyst loadings (Table 3, entry 1 vs 2, 4, 7 and 8 vs 9, 10, 15). Therefore, a loading at 5 mol% of the catalyst with the acid additive could also be used in *aza*-MBH and MBH reactions.

With the conditions optimized, new catalysts **1a**–**f** were tested in *aza*-MBH and MBH reactions in the presence and absence of the 3-methyl benzoic acid additive (Fig. 2). All catalysts require the acid activation to switch on the catalysis. The control reactions without the acid additive demonstrated a sharp reduction in both the reaction rate and the level of enantioselectivity (Fig. 2). Again this concurrent rise of both the enantioselectivity and the reaction rate with acid activation, which is performed at room temperature to maintain the catalytic rate (i.e. no enantioselectivity improvement at lower temperatures), is consistent with our switchable trifunctional catalytic mode as noted before for trifunctional MAP-based catalysts [9,11]. The *aza*-MBH product **14a** of opposite enantioselectivity (up to −35% *ee*) were observed in *aza*-MBH reactions without the acid additive (Fig. 2, **1a, b, d**–**f**).

The substituted pyrrole-containing catalysts **1b** and **1c** (fused benzene ring), compared to the unsubstituted catalyst **1a**, provided higher enantioselectivity in both *aza*-MBH and MBH reactions, albeit in lower reaction rates due to likely higher steric congestion (Fig. 2). The imidazolyl-containing catalysts **1d**–**f** were less active than pyrrolyl-containing analogs with lower reaction rates. The 4-imidazolyl-containing catalyst **1d** showed the lowest activity, resulting in the formation of *aza*-MBH product **14a** in only 41% conversion and 57% *ee* over 3 hours and the MBH product in 48% conversion and 38% *ee* over 6 hours (Fig. 2). As discussed earlier, this may be explained by possible imidazole ring tautomerization that makes the position of the Brønsted acid function less optimal for hydrogen bonding interactions between all catalytic motifs. The imidazole ring tautomerization in catalysts **1e** or **1f** does not seem to influence significantly the catalytic proficiency, as both of the nitrogen centers are in equal α-positions to the methylene bridge. Therefore 2-imidazolyl-containing catalysts **1e** or **1f** provided products in comparable enantioselectivity to that of pyrrolyl-containing catalysts **1a** or **1c**, albeit in lower conversion. This is consistent with our prior observations that increasing the internal Brønsted acid acidity can improve the catalytic activity to a certain point [13c]. Catalyst **1b** was found to be the most active in both *aza*-MBH and MBH test reactions providing products up to 88% *ee* at 89% conversion over 3 hours in the *aza*-MBH case and 73% *ee* at 81% conversion over 6 hours in the MBH case (Fig. 2).

Taking into account the promising activity of new catalysts, the substrate scope of the best catalyst **1b** was investigated in the *aza*-

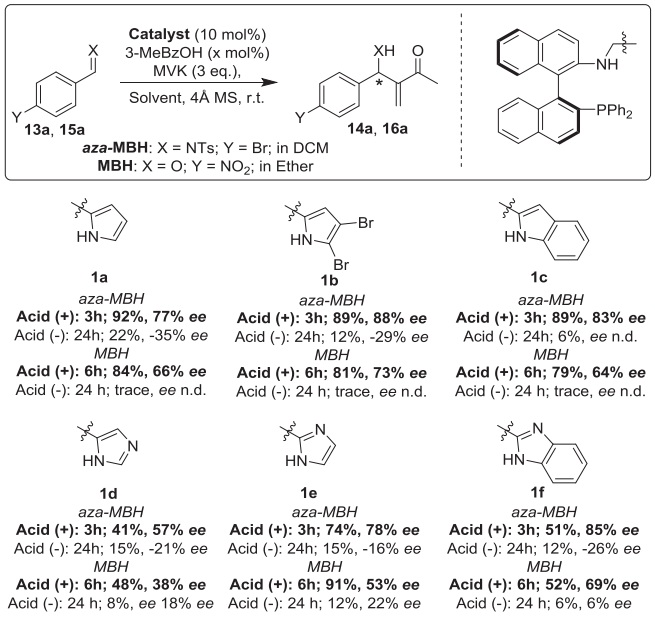

Fig. 2. Activity profile of acid-switchable catalysts **1a**–**f** in *aza*-MBH and MBH test reactions.

Table 3
Acid activator loading screening of **1b**-catalyzed *aza*-MBH and MBH reactions.

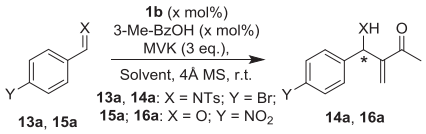

Entry	**1b** loading [mol %]	3-MeBzOH loading [mol %]	X (Y)	Solvent	Time [h]	Conv[a] (*ee*[b]) [%]
1	1	1	NTs (Br)	DCM	3	19 (*88*)
2	5	5	NTs (Br)	DCM	3	57 (*86*)
3	10	5	NTs (Br)	DCM	3	76 (*84*)
4	10	10	NTs (Br)	DCM	3	89 (*88*)
5	10	25	NTs (Br)	DCM	3	49 (*78*)
6	10	50	NTs (Br)	DCM	3	24 (*75*)
7	20	20	NTs (Br)	DCM	3	>95 (*84*)
8	1	1	O (NO_2)	Ether	24	14 (67)
9	5	5	O (NO_2)	Ether	6	70 (*69*)
10	10	10	O (NO_2)	Ether	6	81 (*73*)
11	10	5[c]	O (NO_2)	Ether	6	66 (*63*)
12	10	10[c]	O (NO_2)	Ether	6	62 (*73*)
13	10	25[c]	O (NO_2)	Ether	6	46 (*74*)
14	10	50[c]	O (NO_2)	Ether	6	35 (*74*)
15	20	20	O (NO_2)	Ether	3	>95 (*72*)

[a] Calculated by ^{1}H NMR spectroscopy.
[b] Determined by chiral HPLC analysis.
[c] 2-Naphthoic acid was used instead of 3-methyl benzoic acid.

Table 4
Substrate scope investigation with **1b**.

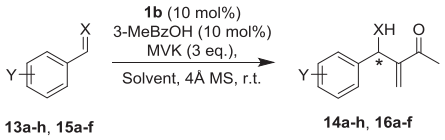

Entry	X (Y)	Solvent	Time [h]	Conv[a] [%]	*ee*[b] [%]
1	NTs (4-Br) **14a**	DCM	3	89 (>95[c])	88
2	NTs (3-NO_2) **14b**	DCM	3	>95	77
3	NTs (2-Cl) **14c**	DCM	3	40 (>95[c])	76
4	NTs (4-Me) **14d**	DCM	3	18 (86[c])	86[d]
5	NTs (2-NO_2) **14e**	DCM	3	53 (>95[c])	58
6	NTs (4-Cl) **14f**	DCM	3	59 (>95[c])	82
7	NTs (4-F) **14g**	DCM	3	21 (>95[c])	79
8	NTs (4-CN) **14h**	DCM	3	55 (>95[c])	57
9	O (4-NO_2) **16a**	Ether	6	81 (>95[c])	73
10	O (3-NO_2) **16b**	Ether	6	68 (>95[c])	73
11	O (4-CN) **16c**	Ether	6	64 (95[c])	73
12	O (4-Br) **16d**	Ether	6	16 (56[c])	75[d]
13	O (2-NO_2) **16e**	Ether	6	14 (58[c])	59[d]
14	O (3-Br) **16f**	Ether	6	10 (48[c])	77[d]

[a] Calculated by ^{1}H NMR spectroscopy.
[b] Determined by chiral HPLC analysis.
[c] Conversion in 24 h.
[d] *ee* level determined for conversion after 24 h.

MBH and MBH reaction (Table 4). Substituted *N*-tosyl benzaldimines with *ortho*-, *meta*-, and *para*-substituents and aromatic aldehydes bearing electron-withdrawing groups were investigated under the optimized conditions.

Catalyst **1b** catalyzed both *aza*-MBH and MBH reactions and demonstrated the widest scope in all of our generations of trifunctional organocatalysts. Most of the *aza*-MBH substrates, containing *para*-substituents, provided the corresponding adducts in comparable enantioselectivity (79–88% *ee*) although with lower conversion for deactivated imine **13d** as expected (Table 4, entries 4 vs. 1). The *aza*-MBH reactions with substrates containing *meta*- and *ortho*-substituents (Table 4, entries 2, 3, 5) showed some loss in enantioselectivity or rate, again consistent with prior observations for substrates that are more sterically congested.

For the MBH reactions, aromatic substrates bearing electron-withdrawing groups provided adducts with consistent *ee* around 73–77% (Table 4. Entries 9–11). Less active 4-bromo- or 3-bromo-substituted aldehydes (**15d** or **15f**) demonstrated only 10–16% conversion in 6 h but longer reaction time to 24 h improved conversion significantly without *ee* erosion (Table 4, entries 12, 14). Substrates with larger *ortho*-substitution, such as imine **14e** and aldehyde **15e**, provided reduced reaction rate and enantioselectivity, suggesting unfavorable steric interactions at that position (Table 4, entries 5 and 13). To date there have been many proficient catalysts reported for the *aza*-MBH or MBH reactions [12f], however, only a few can demonstrate good proficiency in both reactions, due to the very complex mechanisms behind this reaction class [12f]. Bifunctional catalyst β-isocupreidine (β-ICD) provided *aza*-MBH [26] products in up to 99% *ee* and 54–80% yield over 24–36 h at −30 °C, but demonstrated significantly lower proficiency in MBH [27] product formation (up to 49% *ee* and 43–88% yield over 72 h at −30 °C), except for very reactive isatins [28] or 1,1,1,3,3,3-hexafluoroisopropyl acrylate (HFIPA) [29] as an activated alkene. Other examples of bifunctional catalytic systems, active in both *aza*-MBH and MBH reactions between MVK and aromatic electrophiles are MOP-based Shi's [30] and He's [31] catalysts that demonstrated low proficiency in MBH despite the promising activity in the *aza*-MBH analogs. The chiral proline/imidazole catalytic system was also used for proficient catalysis of both *aza*-MBH [32] and MBH [33] reactions, however, substrates such as MVK and aromatic electrophiles were not tested with this catalytic system. The ability of pyrrolyl-containing catalyst **1b** to catalyze both *aza*-MBH and MBH reactions with expanded substrate scope is suggestive of an enhanced molecular recognition network provided by the pyrrole motif in the presence of 3-methyl benzoic acid and encouraging for future work of catalyst design that may help find additional solutions to the generality limitation of this type of reactions.

3. Conclusions

In conclusion, new catalytic roles of a pyrrole motif have been established in a switchable and enantioselective trifunctional organocatalytic cycle that improved the generality of the catalytic systems. Such improvement may be attributed to additional, favourable CH/π hydrogen bonding interactions between the electron rich pyrrolyl moiety and the external activator, 3-methyl benzoic acid to switch on the catalysis. While pyrrole phosphines have commonly been used as ligands before, we show here for the first time that they can be effective organocatalysts. This will facilitate future work in developing the pyrrole motif in catalysis beyond its common ligand role. Further work will involve additional investigation and characterization of substituted pyrroles and acid switches with compact molecular recognition network for new or enhanced catalysis. This may also, in general, contribute to the new use of pyrroles for building molecular assemblies in roles different from the established utility as a coordination or pH-switching site.

4. Experimental section

4.1. General information

All reagents unless specified otherwise are commercially available and purified by standard procedures [34]. Chloroform-*d* was purchased from Cambridge Isotope Laboratories, USA and stored over anhydrous potassium carbonate before use. Bromomethyl methyl ether was distilled from anhydrous sodium sulfate and used immediately after distillation. Cesium carbonate was dried before reactions. Air and moisture sensitive reactions were performed under a nitrogen atmosphere. Reactions were magnetically stirred and monitored by thin-layer chromatography (TLC) using Merck silica gel 60 F_{254} aluminium pre-coated plates (0.25 mm). Flash column chromatography was performed on Merck silica gel 60 (0.015–0.040 mm). ^{1}H, ^{13}C, and ^{31}P experiments were performed at 298 K on either a Bruker DPX 400 MHz spectrometer equipped with a 5 mm QNP probe. Chemical shifts were reported in ppm using the residual $CHCl_3$ peak as an internal reference ($\delta_H = 7.26$ ppm, $\delta_C = 77.16$ ppm). All ^{31}P NMR spectroscopy was performed on a Bruker DPX 400 MHz spectrometer at 298 K, and all spectra were referenced to external H_3PO_4 (0 ppm). All spectra were processed using Bruker TOPSPIN software versions 3.5pl7. Infrared spectra were taken on Thermo Scientific Nicolet iS5FT-IR Spectrometer with an attenuated total reflectance (ATR) accessory and maximum absorption peaks were reported in cm^{-1}. High-resolution mass analysis was provided by Australian Proteome Analysis Facility (APAF), Macquarie University, Sydney, Australia. Chiral HPLC analysis was performed using a Shimadzu Prominence system with either a Daicel Chiral Columns CHIRALPAK® AD–H column or a Regis Chiral Technologies Whelk-O1 column. HPLC grade solvents were degassed before use. Specific rotation was measured at 23–24 °C on a P1010 digital polarimeter (Jasco, Japan). The commercially available aldehydes were used for catalysts synthesis

except for 4,5-dibromopyrrole-2-carboxaldehyde **4** that was obtained [35] via the bromination of pyrrole-2-carboxaldehyde **3**. (*S*)-MAPO **6** and aminophosphine **2** were synthesized by established procedures [9,24]

4.2. Experimental details

4.2.1. General procedure for MBH or aza-MBH reactions

Catalyst (10 mol%, 0.0025 mmol), imine or aldehyde (0.025 mmol) and acid additive (10 mol%, 0.0025 mmol) were combined under N_2 from dichloromethane stock solutions in a 1.5 mL teflon capped vial with 4 Å molecular sieves. Dichloromethane was evaporated by nitrogen flow. Then reaction solvent was added to the mixture (final concentration C = 0.2 M to imine or aldehyde after addition of MVK in the reaction solvent). A solution of MVK (0.075 mmol) was added to the mixture at stirring at room temperature. Aliquots (10 μL) of the reaction mixture were taken at 0.5, 3, 6, 24 h and dried immediately by nitrogen flow to remove the volatiles. The residue was re-dissolved in chloroform-*d* and filtered to determine the conversion of starting material to product by ^{1}H NMR and then analyzed by chiral HPLC (1:4 *i*-propanol:hexane) to determine *ee* ratios.

4.2.2. (S)-N-((1H-pyrrol-2-yl)methyl)-2′-(diphenylphosphaneyl)-[1,1′-binaphthalen]-2-amine (**1a**)

To a solution of (*S*)-(+)-2-(diphenylphosphine)-1,1′-binaphthyl-2′-amine **2** (100 mg, 0.221 mmol) and 2-pyrrolecarboxaldehyde (42 mg, 0.441 mmol) in dry toluene (4 mL) was added a drop of formic acid at room temperature and the reaction mixture was stirred for 15 h. The mixture was pre-cooled (ice/NaCl bath) and dry methanol (15 μL) was added followed by the addition of $NaBH_4$ (21 mg, 0.551 mmol) in one portion and stirred at room temperature for 10 min. The mixture was treated with water and the organic phase was extracted by dichloromethane 3 times. The combined organic phases were washed with brine, dried over anhydrous magnesium sulfate and concentrated under vacuum. The residue was purified by flash chromatography on silica gel (toluene; crude mixture/SiO_2 as 1/250 w/w) to furnish **1a** (28 mg, 24% yield) as a white solid. ^{1}H NMR (400 MHz, $CDCl_3$) δ 3.72 (bs, 1H), 4.15–4.28 (m, 2H), 5.93–5.98 (m, 1H), 6.05–6.10 (m, 1H), 6.44–6.50 (m, 1H), 6.53 (d, J = 8.0 Hz, 1H), 6.87–6.94 (m, 1H), 6.97–7.03 (m, 2H), 7.05–7.20 (m, 5H), 7.24–7.38 (m, 7H), 7.44 (dd, J = 2.9, 8.6 Hz, 1H), 7.49–7.55 (m, 1H), 7.69 (d, J = 8.0 Hz, 1H), 7.81 (d, J = 8.9 Hz, 1H), 7.91 (d, J = 8.5 Hz, 1H), 7.92 (d, J = 8.2 Hz, 1H), 8.23 (bs, 1H); ^{31}P NMR (162 MHz, $CDCl_3$) δ −13.06; ^{13}C NMR (100 MHz, $CDCl_3$) δ 41.59, 104.80, 108.43, 113.59, 116.97, 121.88, 124.22, 125.44, 126.25, 126.33 (d, J_{C-P} = 2.2 Hz), 127.09, 127.36, 127.90, 128.23, 128.30, 128.35, 128.37, 128.50, 128.64, 128.68, 128.78, 128.84, 129.18, 129.93 (d, J_{C-P} = 2.9 Hz), 130.69 (d, J_{C-P} = 1.5 Hz), 133.61 (d, J_{C-P} = 8.07 Hz), 133.81 (d, J_{C-P} = 8.5 Hz), 134.02 (d, J_{C-P} = 2.2 Hz), 134.41, 137.75, 141.43, 141.78, 143.42 (d, J_{C-P} = 2.2 Hz); IR (ATR, cm^{-1}) ν 3427, 3051, 1618, 1596, 1511, 1492, 1430, 1332, 1298, 1255, 1214, 1151, 1089, 1024; HRMS Found $[M+H]^+$, 533.21356. $C_{37}H_{30}N_2P$ requires $[M+H]^+$, 533.21466; $[\alpha]_D^{23}$ -15.94 (*c* 1.0, $CHCl_3$).

4.2.3. (S)-N-((4,5-dibromo-1H-pyrrol-2-yl)methyl)-2′-(diphenylphosphaneyl) -[1,1′-binaphthalen]-2-amine (**1b**)

To a solution of (*S*)-(+)-2-(diphenylphosphine)-1,1′-binaphthyl-2′-amine **2** (56 mg, 0.124 mmol) and 4,5-dibromo-2-pyrrolecarboxaldehyde (63 mg, 0.248 mmol) in dry toluene (2.3 mL) was added a drop of formic acid at room temperature and the reaction mixture was stirred for 4.5 h. The mixture was pre-cooled (ice/acetone bath) and dry methanol (15 μL) was added followed by the addition of $NaBH_3CN$ (15.5 mg, 0.247 mmol) in one portion and stirred at room temperature for 7.5 h. The mixture was treated with water and the organic phase was extracted by dichloromethane 3 times. The combined organic phases were washed with brine, dried over anhydrous magnesium sulfate and concentrated under vacuum. The residue was purified by flash chromatography on silica gel (hexane/dichloromethane gradient) to furnish **1b** (44 mg, 51% yield) as a white solid. ^{1}H NMR (400 MHz, $CDCl_3$) δ 3.92 (bs, 1H), 4.18–4.34 (m, 2H), 5.96–6.12 (m, 1H), 6.36 (d, J = 8.5 Hz, 1H), 6.73–6.81 (m, 1H), 6.94–7.13 (m, 7H), 7.21–7.33 (m, 4H), 7.34–7.39 (m, 3H), 7.42 (dd, J = 3.3, 8.5 Hz, 1H), 7.49–7.55 (m, 1H), 7.62 (d, J = 8.0 Hz, 1H), 7.79 (d, J = 8.9 Hz, 1H), 7.92 (d, J = 8.6 Hz, 1H), 7.93 (d, J = 8.1 Hz, 1H), 9.74 (bs, 1H); ^{31}P NMR (162 MHz, $CDCl_3$) δ −12.38; ^{13}C NMR (100 MHz, $CDCl_3$) δ 41.08, 98.21, 108.20, 113.25, 121.99, 124.28, 126.09 (d, J_{C-P} = 2.2 Hz), 126.20, 127.22, 127.36, 127.42, 127.71, 128.19, 128.27, 128.38, 128.73 (d, J_{C-P} = 1.5 Hz), 128.85, 128.91 (d, J_{C-P} = 2.2 Hz), 130.07, 130.19, 131.70, 133.20, 133.57, 133.76, 134.08, 134.29, 134.36, 136.47 (d, J_{C-P} = 8.1 Hz), 136.99 (d, J_{C-P} = 6.6 Hz), 141.69; IR (ATR, cm^{-1}) ν 3416, 3051, 1617, 1596, 1512, 1492, 1431, 1293, 1254, 1152, 1092, 1024, 968; HRMS Found $[M+H]^+$, 691.03129. $C_{37}H_{28}Br_2N_2P$ requires $[M+H]^+$, 691.03364; $[\alpha]_D^{23}$ -41.98 (*c* 0.77, $CHCl_3$).

4.2.4. (S)-N-((1H-indol-2-yl)methyl)-2′-(diphenylphosphaneyl)-[1,1′-binaphthalen]-2-amine (**1c**)

To a solution of (*S*)-(+)-2-(diphenylphosphine)-1,1′-binaphthyl-2′-amine **2** (50 mg, 0.11 mmol) and 2-indolecarboxaldehyde (48 mg, 0.331 mmol) in dry toluene (2 mL) was added a drop of formic acid at room temperature and the reaction mixture was stirred for 15 h. The mixture was pre-cooled (ice/acetone bath) and dry methanol (134 μL, 3.308 mmol) was added followed by the addition of $NaBH_3CN$ (69.3 mg, 1.103 mmol, 10 eq) in one portion and stirred 40 °C for 3.5 h. The mixture was treated with water and the organic phase was extracted by dichloromethane 3 times. The combined organic phases were washed with brine, dried over anhydrous magnesium sulfate and concentrated under vacuum. The residue was purified by flash chromatography on silica gel (hexane/dichloromethane gradient) to furnish **1c** (45 mg, 70% yield) as a white solid. ^{1}H NMR (400 MHz, $CDCl_3$) δ 3.92 (bs, 1H), 4.34–4.51 (m, 2H), 6.28–6.35 (m, 1H), 6.50 (d, J = 8.5 Hz, 1H), 6.83–6.91 (m, 1H), 6.99–7.20 (m, 10H), 7.29–7.40 (m, 7H), 7.47 (dd, J = 3.0, 8.5 Hz, 1H), 7.50–7.57 (m, 2H), 7.66 (d, J = 8.0 Hz, 1H), 7.76 (d, J = 8.9 Hz, 1H), 7.93 (d, J = 8.5 Hz, 1H), 7.94 (d, J = 8.2 Hz, 1H), 8.82 (bs, 1H); ^{31}P NMR (162 MHz, $CDCl_3$) δ −13.01; ^{13}C NMR (100 MHz, $CDCl_3$) δ 41.82, 98.73, 111.02, 113.51, 119.67, 120.02, 121.19, 121.97, 124.26, 126.25, 127.14, 127.37, 127.43, 127.83, 128.25, 128.32, 128.41, 128.69, 128.75, 128.86, 128.92, 129.02, 130.06, 130.41, 133.16 (d, J_{C-P} = 7.2 Hz), 133.52, 133.71, 133.88, 133.93 (d, J_{C-P} = 2.2 Hz), 134.08, 134.41, 135.80, 135.87, 135.96, 137.26, 137.36 (d, J_{C-P} = 2.9 Hz), 137.52, 141.10, 141.43, 142.80; IR (ATR, cm^{-1}) ν 3416, 3050, 1886, 1618, 1596, 1512, 1490, 1455, 1430, 1339, 1292, 1216, 1152, 1091, 1023; HRMS Found $[M+H]^+$, 583.22877. $C_{41}H_{32}N_2P$ requires $[M+H]^+$, 583.23031; $[\alpha]_D^{23}$ -122.07 (*c* 1.0, $CHCl_3$).

4.2.5. (S)-(2′-(((1H-imidazol-5-yl)methyl)amino)-[1,1′-binaphthalen]-2-yl)diphenylphosphine oxide (**10**)

A mixture of (*S*)-(+)-2-(diphenylphosphine oxide)-1,1′-binaphthyl-2′-amine **6** (150 mg, 0.320 mmol) and 4(5)-formylimidazole (61.4 mg, 0.640 mmol) in the presence of 4 Å molecular sieves (0.7 g) in dry toluene (5.8 mL) was stirred at 110 °C for 17 h in a pressure tube. The mixture was cooled down to room temperature and then pre-cooled (ice/NaCl bath). After cooling, dry methanol (0.5 mL) was added and then $NaBH_3CN$ (20 mg, 0.320 mmol) was added in one portion and stirred at room temperature for 2.5 h. The mixture was filtered through folded filter.

The reaction mixture was treated with water and the organic phase was extracted with ethyl acetate (3 times). The combined organic phases were washed with brine, dried over anhydrous magnesium sulfate and concentrated under vacuum. The residue was purified by flash chromatography on silica gel (1–10% ethanol in chloroform; gradient) to furnish **10** (119.1 mg, 68% yield) as yellow foam. ^{1}H NMR (400 MHz, $CDCl_3$) δ 4.06 (bs, 1H), 4.33–4.43 (m, 1H), 4.52–4.62 (m, 1H), 6.32 (d, J = 8.3 Hz, 1H), 6.61–6.70 (m, 2H), 6.78–6.88 (m, 2H), 6.91–6.98 (m, 1H), 6.96 (d, J = 9.0 Hz, 1H), 7.00 (s, 1H), 7.02–7.11 (m, 2H), 7.22 (d, J = 8.3 Hz, 1H), 7.26–7.33 (m, 1H), 7.36 (d, J = 7.9 Hz, 1H), 7.48 (d, J = 8.9 Hz, 1H), 7.50–7.65 (m, 5H), 7.70 (s, 1H), 7.87–8.00 (m, 4H). ^{31}P NMR (162 MHz, $CDCl_3$) δ 28.16; ^{13}C NMR (100 MHz, $CDCl_3$) δ 39.41, 113.23, 113.83 (d, J_{C-P} = 5 Hz), 121.44, 124.23, 126.00, 126.65, 127.19, 127.25, 127.32, 127.83, 128.32, 128.55, 128.64, 128.67, 128.73, 128.85, 128.92, 129.10, 129.24, 129.62, 129.71, 129.72, 130.12 (d, J = 2.3 Hz), 130.53, 130.59, 131.56, 132.01, 132.05, 132.10, 132.37, 133.41, 133.52, 135.68 (dd, J_{C-P} = 8.8, 2.2 Hz), 141.8 (d, J_{C-P} = 9.5 Hz), 144.42; IR (ATR, cm^{-1}) ν 3054, 1618, 1597, 1497, 1435, 1342, 1301, 1258, 1215, 1153, 1112; HRMS Found $[M+H]^+$, 550.20391. $C_{36}H_{29}N_3OP$ requires $[M+H]^+$, 550.20483; $[\alpha]_D^{24}$ +80.83 (c 1.0, $CHCl_3$).

4.2.6. (S)-N-((1H-imidazol-5-yl)methyl)-2′-(diphenylphosphaneyl)-[1,1′-binaphthalen]- 2-amine (**1d**)

A solution of **10** (70.5 mg, 0.128 mmol) in neat phenylsilane (80 μL) was heated at 96 °C for 19 hours. The volatiles were removed via nitrogen blow down and the residue was purified by flash chromatography on silica gel (hexane/ethyl acetate to ethyl acetate/ethanol; gradient) to yield **1d** (36.3 mg, 53%) as a white foam. ^{1}H NMR (400 MHz, $CDCl_3$) δ 3.76 (bs, 1H), 4.21 (s, 2H), 6.53 (d, J = 8.4 Hz, 1H), 6.71–6.75 (m, 1H), 6.86–6.92 (m, 1H), 6.97–7.04 (m, 2H), 7.05–7.20 (m, 6H), 7.21–7.34 (m, 6H), 7.35–7.38 (m, 1H), 7.45 (dd, J = 2.8, 8.6 Hz, 1H), 7.47–7.53 (m, 1H), 7.69 (d, J = 8.0 Hz, 1H), 7.80 (d, J = 8.9 Hz, 1H), 7.90 (d, J = 8.5 Hz, 2H); ^{31}P NMR (162 MHz, $CDCl_3$) δ −13.61; ^{13}C NMR (100 MHz, $CDCl_3$) δ 40.47, 113.44, 116.43 (d, J_{C-P} = 8.7 Hz), 121.89, 124.22, 126.27, 126.40 (d, J_{C-P} = 2.9 Hz), 127.06, 127.29, 127.37, 127.89, 128.25, 128.32, 128.55, 128.60, 128.66, 128.71, 128.77, 129.84, 130.69, 133.08 (d, J_{C-P} = 7.0 Hz), 133.40, 133.59, 133.70, 133.90, 134.09 (d, J_{C-P} = 2.2 Hz), 134.39, 134.54, 136.62 (d, J_{C-P} = 11.5 Hz), 137.22 (d, J_{C-P} = 9.5 Hz), 137.79 (d, J_{C-P} = 12.5 Hz), 141.43, 141.76, 142.97 (d, J_{C-P} = 2.2 Hz); IR (ATR, cm^{-1}) ν 3051, 1618, 1596, 1492, 1430, 1340, 1301, 1251, 1214, 1150, 1088; HRMS Found $[M+H]^+$, 534.20872. $C_{36}H_{29}N_3P$ requires $[M+H]^+$, 534.20991; $[\alpha]_D^{23}$ -2.68 (c 1.0, CH_2Cl_2).

4.2.7. (S)-(2′-(((1H-imidazol-2-yl)methyl)amino)-[1,1′-binaphthalen]-2-yl)diphenylphosphine oxide (**11**)

The mixture of (*S*)-(+)-2-(diphenylphosphine oxide)-1,1′-binaphthyl-2′-amine **6** (200 mg, 0.426 mmol) and 2-formylimidazole (82 mg, 0.852 mmol) in the presence of 4 Å MS (0.85 g) in dry toluene (8 mL) was stirred at 110 °C for 70 h in a pressure tube. The mixture was cooled down to room temperature and then pre-cooled (ice/NaCl bath). After cooling, dry methanol (2 mL) was added and then $NaBH_4$ (80 mg, 2.13 mmol) was added in one portion and stirred at room temperature for 3 h. The mixture was filtered through folded filter. The reaction mixture was treated with water and the organic phase was extracted with ethyl acetate (3 times). The combined organic phases were washed with brine, dried over anhydrous magnesium sulfate and concentrated under vacuum. The residue was purified by flash chromatography on silica gel (toluene/ethyl acetate to ethyl acetate; gradient) to furnish **11** (80.4 mg, 34.3% yield) as yellow foam. ^{1}H NMR (400 MHz, $CDCl_3$) δ 4.23 (t, J = 6.5 Hz, 1H), 4.46 (dd, J = 6.1, 17.5 Hz, 1H), 5.20 (dd, J = 7.1, 17.5 Hz, 1H), 6.23 (d, J = 8.4 Hz, 1H), 6.69–6.77 (m, 3H), 6.85–6.95 (m, 3H), 7.05–7.14 (m, 4H), 7.25 (d, J = 8.5 Hz, 1H), 7.28–7.34 (m, 1H), 7.37 (d, J = 8.0 Hz, 1H), 7.48–7.63 (m, 6H), 7.84–8.00 (m, 4H), 13.40 (bs, 1H); ^{31}P NMR (162 MHz, $CDCl_3$) δ 28.17; ^{13}C NMR (100 MHz, $CDCl_3$) δ 41.48, 112.39, 113.95 (d, J_{C-P} = 5.1 Hz), 121.49, 124.11, 126.00, 126.72, 127.12, 127.48, 127.60, 127.78, 128.02, 128.32, 128.47, 128.54, 128.67, 128.79, 128.91, 129.04, 129.09, 129.17, 129.53, 129.95, 130.05, 130.53 (d, J_{C-P} = 2.9 Hz), 130.72, 132.07, 132.15, 132.33, 133.12, 133.41, 133.52 (d, J_{C-P} = 10.3 Hz), 135.71 (d, J_{C-P} = 2.2 Hz), 142.00 (d, J_{C-P} = 8.7 Hz), 143.58, 147.54; IR (ATR, cm^{-1}) ν 3053, 1618, 1598, 1551, 1498, 1436, 1300, 1178, 1155, 1113, 1096, 1024, 998, 869, 810, 744, 722, 696, 633; HRMS Found $[M+H]^+$, 550.20362. $C_{36}H_{29}N_3OP$ requires $[M+H]^+$, 550.20483; $[\alpha]_D^{23}$ 33.25 (c 1.0, $CHCl_3$).

4.2.8. (S)-N-((1H-imidazol-2-yl)methyl)-2′-(diphenylphosphaneyl)-[1,1′-binaphthalen]-2-amine (**1e**)

A solution of **11** (18.1 mg, 0.033 mmol) in neat phenylsilane (200 μL) was heated at 90 °C for 68 hours. The volatiles were removed via nitrogen blow down and the residue was purified by flash chromatography on silica gel (hexane/ethyl acetate; gradient) to yield **1e** (8.1 mg, 46%) as a white foam. ^{1}H NMR (400 MHz, $CDCl_3$) δ 4.02 (t, J = 5.8 Hz, 1H), 4.34 (dd, J = 6.3, 17.5 Hz, 1H), 4.59 (dd, J = 5.3, 17.5 Hz, 1H), 6.41 (d, J = 8.5 Hz, 1H), 6.79–6.90 (m, 3H), 6.92–7.00 (m, 3H), 7.02–7.10 (m, 3H), 7.11–7.17 (m, 1H), 7.23–7.38 (m, 7H), 7.40 (dd, J = 3.2, 8.5 Hz, 1H), 7.50–7.57 (m, 1H), 7.65 (d, J = 8.1 Hz, 1H), 7.78 (d, J = 9.0 Hz, 1H), 7.93 (d, J = 8.4 Hz, 2H); ^{31}P NMR (162 MHz, $CDCl_3$) δ −12.79; ^{13}C NMR (100 MHz, $CDCl_3$) δ 42.01, 112.88, 116.38 (d, J_{C-P} = 8.6 Hz), 122.14, 124.18, 126.16 (d, J_{C-P} = 2.2 Hz), 127.37, 127.30, 127.48, 127.51, 127.82, 128.30, 128.38, 128.40, 128.85, 128.94, 128.96, 129.03, 130.26, 133.13 (d, J_{C-P} = 7.2 Hz), 133.33, 133.52, 133.92 (d, J = 2.2 Hz), 133.97, 134.18, 134.434, 135.00 (d, J_{C-P} = 7.3 Hz), 136.68 (d, J_{C-P} = 6.7 Hz), 136.88 (d, J_{C-P} = 9.4 Hz), 140.87, 141.19, 141.84 (d, J_{C-P} = 2.2 Hz), 147.00; IR (ATR, cm^{-1}) ν 3050, 1618, 1596, 1511, 1493, 1431, 1295, 1262, 1215, 1151, 1091, 1023, 996, 914,852, 810, 773, 739, 694, 629; HRMS Found $[M+H]^+$, 534.20915. $C_{36}H_{29}N_3P$ requires $[M+H]^+$, 534.20991; $[\alpha]_D^{23}$ -55.16 (c 1.0, CH_2Cl_2).

4.2.9. (S)-(2′-(((1H-benzo[d]imidazol-2-yl)methyl)amino)-[1,1′-binaphthalen]-2-yl)diphenylphosphine oxide (**12**)

A mixture of (*S*)-(+)-2-(diphenylphosphine oxide)-1,1′-binaphthyl-2′-amine **6** (200 mg, 0.426 mmol) and 2-formyl-1H-benzoimidazole (187 mg, 1.278 mmol) in the presence of 4 Å MS (0.85 g) in dry toluene (8 mL) was stirred at 110 °C for 14 h in a pressure tube. The mixture was cooled down to room temperature and then pre-cooled (ice/NaCl bath). After cooling, dry methanol (3 mL) was added and then $NaBH_4$ (54 mg, 1.43 mmol) was added in one portion and stirred at room temperature for 1 h. The mixture was filtered through folded filter. The reaction mixture was treated with water and the organic phase was extracted with ethyl acetate (3 times). The combined organic phases were washed with brine, dried over anhydrous magnesium sulfate and concentrated under vacuum. The residue was purified by flash chromatography on silica gel (20–50% of hexane in ethyl acetate; gradient) to furnish **12** (212 mg, 83% yield) as yellow foam. The sample for analysis was recrystallised from toluene/hexane. ^{1}H NMR (400 MHz, $CDCl_3$) δ 4.38 (t, J = 6.6 Hz, 1H), 4.63 (dd, J = 6.3, 18.0 Hz, 1H), 4.88 (dd, J = 7.0, 18.0 Hz, 1H), 6.30 (d, J = 8.4 Hz, 1H), 6.62–6.70 (m, 2H), 6.74–6.80 (m, 1H), 6.82–6.95 (m, 3H), 7.08–7.38 (m, 7H), 7.44 (d, J = 9.0 Hz, 1H), 7.50–7.67 (m, 6H), 7.76 (d, J = 7.9 Hz, 1H), 7.93–8.06 (m, 4H), 13.99 (bs, 1H); ^{31}P NMR (162 MHz, $CDCl_3$) δ −27.87; ^{13}C NMR (100 MHz, $CDCl_3$) δ 42.60, 111.75, 112.54, 113.89 (d, J_{C-P} = 5.1 Hz), 118.72, 121.46, 121.89, 124.23, 125.44, 125.95, 126.65, 127.20, 127.43, 127.55, 127.80, 127.94, 128.35, 128.77, 128.89, 129.00,

129.09, 129.68, 129.78, 130.23 (d, $J_{C-P}=3.8$ Hz), 130.72, 132.07 (d, $J_{C-P}=2.2$ Hz), 132.11, 132.20, 133.25, 133.48, 133.52, 133.59, 135.75 (d, $J_{C-P}=2.2$ Hz), 142.01, 143.86, 154.91; IR (ATR, cm^{-1}) ν 3052, 1619, 1597, 1507, 1434, 1300, 1269, 1220, 1175, 1154, 1113; HRMS Found $[M+H]^+$, 600.21910. $C_{40}H_{31}N_3OP$ requires $[M+H]^+$, 600.22048; $[\alpha]_D^{23}$ -117.44 (*c* 1.0, $CHCl_3$).

4.2.10. (S)-N-((1H-benzo[d]imidazol-2-yl)methyl)-2′-(diphenylphosphaneyl)-[1,1′-binaphthalen]-2-amine (**1f**)

A solution of **12** (40 mg, 0.067 mmol) in neat phenylsilane (300 μL) was heated at 110 °C for 14 hours. The volatiles were removed by nitrogen flow and the residue was purified by flash chromatography on silica gel (20–40% of hexane in ethyl acetate; gradient) to yield **1f** (32.8 mg, 84% yield) as white foam. ^{1}H NMR (400 MHz, $CDCl_3$) δ 4.18 (t, $J=5.9$ Hz, 1H), 4.55 (dd, $J=6.5$, 18.0 Hz, 1H), 4.77 (dd, $J=5.4$, 18.0 Hz, 1H), 6.40 (d, $J=8.5$ Hz, 1H), 6.76–6.84 (m, 1H), 6.96–7.08 (m, 6H), 7.10–7.20 (m, 3H), 7.28–7.40 (m, 9H), 7.45 (dd, $J=3.4$, 8.5 Hz, 1H), 7.51–7.57 (m, 1H), 7.61 (d, $J=8.0$ Hz, 1H), 7.73 (d, $J=9.0$ Hz, 1H), 7.94 (d, $J=8.2$ Hz, 1H), 7.95 (d, $J=8.6$ Hz, 1H), 10.52 (bs, 1H); ^{31}P NMR (162 MHz, $CDCl_3$) δ −12.52; ^{13}C NMR (100 MHz, $CDCl_3$) δ 42.02, 112.61, 116.54 (d, $J_{C-P}=8.2$ Hz), 122.30, 122.95, 124.27, 126.08 (d, $J_{C-P}=2.2$ Hz), 126.43, 127.40, 127.58, 127.62, 127.78, 128.34, 128.42, 128.99, 129.09, 129.15, 129.94, 130.52, 133.17, 133.26, 133.44, 133.87 (d, $J_{C-P}=1.5$ Hz), 134.06, 134.12, 134.33, 134.44, 136.25 (d, $J_{C-P}=6.6$ Hz), 136.67 (d, $J_{C-P}=5.1$ Hz), 140.55, 140.86, 141.13 (d, $J_{C-P}=2.2$ Hz), 153.71 (d, $J_{C-P}=1.5$ Hz); IR (ATR, cm^{-1}) ν 3051, 1618, 1596, 1511, 1492, 1452, 1428, 1323, 1293, 1266, 1216, 1151, 1092, 1023, 998, 951, 917, 845, 809, 737, 694, 628. HRMS Found $[M+H]^+$, 584.22415. $C_{40}H_{31}N_3P$ requires $[M+H]^+$, 584.22556; $[\alpha]_D^{23}$ -126.95 (*c* 1.0, CH_2Cl_2).

Acknowledgements

We are grateful to Macquarie University for an iMQRES scholarship to SE.

Appendix A. Supplementary data

Supplementary data to this article can be found online at https://doi.org/10.1016/j.tet.2018.12.016.

References

[1] a) A. Domagala, T. Jarosz, M. Lapkowski, Eur. J. Med. Chem. 100 (2015) 176–187;
b) S. Said Fatahala, S. Hasabelnaby, A. Goudah, G. Mahmoud, R. Helmy Abd-El Hameed, Molecules 22 (2017) 461;
c) E. Yasui, M. Wada, N. Takamura, Tetrahedron Lett. 50 (2009) 4762–4765;
d) A. Aiello, E. Fattorusso, A. Giordano, M. Menna, W.E.G. Müller, S. Perović-Ottstadt, H.C. Schröder, Bioorg. Med. Chem. 15 (2007) 5877–5887.

[2] a) N. Grüger, H. Wadepohl, L.H. Gade, Dalton Trans. 41 (2012) 14028–14030;
b) A. Gualandi, L. Cerisoli, H. Stoeckli-Evans, D. Savoia, J. Org. Chem. 76 (2011) 3399–3408;
c) C.A. Caputo, N.D. Jones, Dalton Trans. (2007) 4627–4640;
d) C. Mazet, L.H. Gade, Chem. Eur. J. 8 (2002) 4308–4318.

[3] a) H. Maeda, Y. Kusunose, Chem. Eur. J. 11 (2005) 5661–5666;
b) R. Yamakado, Y. Ashida, R. Sato, Y. Shigeta, N. Yasuda, H. Maeda, Chem. Eur. J. 23 (2017) 4160–4168;
c) A. Kuno, N. Tohnai, N. Yasuda, H. Maeda, Chem. Eur. J. 23 (2017) 11357–11365;
d) Y. Haketa, Y. Bando, K. Takaishi, M. Uchiyama, A. Muranaka, M. Naito, H. Shibaguchi, T. Kawai, H. Maeda, Angew. Chem. Int. Ed. 51 (2012) 7967–7971;
e) H. Maeda, Y. Bando, K. Shimomura, I. Yamada, M. Naito, K. Nobusawa, H. Tsumatori, T. Kawai, J. Am. Chem. Soc. 133 (2011) 9266–9269;
f) H. Maeda, Y. Kusunose, Y. Mihashi, T. Mizoguchi, J. Org. Chem. 72 (2007) 2612–2616;
g) H. Maeda, T. Shirai, Y. Bando, K. Takaishi, M. Uchiyama, A. Muranaka, T. Kawai, M. Naito, Org. Lett. 15 (2013) 6006–6009;
h) Y. Haketa, H. Maeda, Chem. Eur. J. 17 (2011) 1485–1492;
i) H. Maeda, M. Terasaki, Y. Haketa, Y. Mihashi, Y. Kusunose, Org. Biomol. Chem. 6 (2008) 433–436;
j) H. Maeda, Y. Haketa, T. Nakanishi, J. Am. Chem. Soc. 129 (2007) 13661–13674.

[4] a) R. Yamakado, T. Sakurai, W. Matsuda, S. Seki, N. Yasuda, S. Akine, H. Maeda, Chem. Eur. J. 22 (2016) 626–638;
b) B. Dong, T. Sakurai, Y. Honsho, S. Seki, H. Maeda, J. Am. Chem. Soc. 135 (2013) 1284–1287;
c) B. Dong, T. Sakurai, Y. Bando, S. Seki, K. Takaishi, M. Uchiyama, A. Muranaka, H. Maeda, J. Am. Chem. Soc. 135 (2013) 14797–14805;
d) Y. Haketa, Y. Honsho, S. Seki, H. Maeda, Chem. Eur. J. 18 (2012) 7016–7020;
e) Y. Haketa, S. Sasaki, N. Ohta, H. Masunaga, H. Ogawa, N. Mizuno, F. Araoka, H. Takezoe, H. Maeda, Angew. Chem. Int. Ed. 49 (2010) 10079–10083.

[5] M. Nishio, Y. Umezawa, K. Honda, S. Tsuboyama, H. Suezawa, CrystEngComm 11 (2009) 1757–1788.

[6] a) M. Roucan, M. Kielmann, S.J. Connon, S.S.R. Bernhard, M.O. Senge, Chem. Commun. 54 (2018) 26–29;
b) G. Cafeo, M. De Rosa, F.H. Kohnke, P. Neri, A. Soriente, L. Valenti, Tetrahedron Lett. 49 (2008) 153–155;
c) G. Hirata, H. Maeda, Org. Lett. 20 (2018) 2853–2856;
d) M. Kielmann, M.O. Senge, Angew. Chem. Int. Ed. 57 (2018) 2–26, in press;
e) D.S. Kim, J.L. Sessler, Chem. Soc. Rev. 44 (2015) 532–546;
f) G. Aragay, D. Hernández, B. Verdejo, E. Escudero-Adán, M. Martínez, P. Ballester, Molecules 20 (2015) 16672;
g) L. Adriaenssens, C. Estarellas, A. Vargas Jentzsch, M. Martinez Belmonte, S. Matile, P. Ballester, J. Am. Chem. Soc. 135 (2013) 8324–8330;
h) J.R. Blas, J.M. López-Bes, M. Márquez, J.L. Sessler, F.J. Luque, M. Orozco, Chem. Eur. J. 13 (2007) 1108–1116;
i) J.S. Park, C. Bejger, K.R. Larsen, K.A. Nielsen, A. Jana, V.M. Lynch, J.O. Jeppesen, D. Kim, J.L. Sessler, Chem. Sci. 3 (2012) 2685–2689.

[7] a) U. Lüning, Angew. Chem. Int. Ed. 51 (2012) 8163–8165;
b) J. Choudhury, S. Semwal, Synlett 29 (2018) 141–147;
c) E. Peris, Chem. Rev. 11 (8) (2018) 9988–10031;
d) A.J.M. Miller, Dalton Trans. 46 (2017) 11987–12000;
e) V. Blanco, D.A. Leigh, V. Marcos, Chem. Soc. Rev. 44 (2015) 5341–5370;
f) D. Troegel, J. Stohrer, Coord. Chem. Rev. 255 (2011) 1440–1459.

[8] a) N.J. Zondlo, Acc. Chem. Res. 46 (2013) 1039–1049;
b) M. Nishio, Tetrahedron 61 (2005) 6923–6950.

[9] J.-M. Garnier, C. Anstiss, F. Liu, Adv. Synth. Catal. 351 (2009) 331–338.

[10] a) D. Sälinger, R. Brückner, Synlett 2009 (2009) 109–111;
b) T. Ooi, K. Ohmatsu, K. Maruoka, J. Am. Chem. Soc. 129 (2007) 2410–2411;
c) Š. Vyskočil, M. Smrčina, V. Hanuš, M. Polášek, P. Kočovský, J. Org. Chem. 63 (1998) 7738–7748;
d) Y.-L. Yang, C.-K. Pei, M. Shi, Org. Biomol. Chem. 9 (2011) 3349–3358;
e) P.N.M. Botman, O. David, A. Amore, J. Dinkelaar, M.T. Vlaar, K. Goubitz, J. Fraanje, H. Schenk, H. Hiemstra, J.H. van Maarseveen, Angew. Chem. Int. Ed. 43 (2004) 3471–3473.

[11] C. Anstiss, F. Liu, Tetrahedron 66 (2010) 5486–5491.

[12] a) D. Cantillo, C.O. Kappe, J. Org. Chem. 75 (2010) 8615–8626;
b) I.T. Raheem, E.N. Jacobsen, Adv. Synth. Catal. 347 (2005) 1701–1708;
c) K.E. Price, S.J. Broadwater, B.J. Walker, D.T. McQuade, J. Org. Chem. 70 (2005) 3980–3987;
d) P. Buskens, J. Klankermayer, W. Leitner, J. Am. Chem. Soc. 127 (2005) 16762–16763;
e) V.K. Aggarwal, S.Y. Fulford, G.C. Lloyd-Jones, Angew. Chem. Int. Ed. 44 (2005) 1706–1708;
f) R. Kenny, F. Liu, Chem. Rec. 17 (2017) 535–553.

[13] a) R. Kenny, F. Liu, Eur. J. Org. Chem. (2015) 5304–5319;
b) C. Anstiss, J.-M. Garnier, F. Liu, Org. Biomol. Chem. 8 (2010) 4400–4407;
c) J.-M. Garnier, F. Liu, Org. Biomol. Chem. 7 (2009) 1272–1275.

[14] K. Junge, G. Oehme, A. Monsees, T. Riermeier, U. Dingerdissen, M. Beller, J. Organomet. Chem. 675 (2003) 91–96.

[15] a) A.D. Burrows, M.F. Mahon, M. Varrone, Dalton Trans. (2003) 4718–4730;
b) X. Shu, H. Liang, Q. Wu, F. Zhou, X. Zheng, H. Fu, B. Xu, R. Li, C. Zhang, H. Chen, RSC Adv. 7 (2017) 14816–14823;
c) X.-L. Zheng, C.-Y. Zheng, F.-D. Zhou, H.-Y. Fu, M.-L. Yuan, R.-X. Li, B. Xu, H. Chen, Chin. Chem. Lett. 27 (2016) 678–680;
d) R. Luo, H.-r. Liang, X.-l. Zheng, H.-y. Fu, M.-l. Yuan, R.-x. Li, H. Chen, Catal. Commun. 50 (2014) 29–33.

[16] A.M. Brosnahan, A. Talbot, B.A. McKeown, S.E. Kalman, T.B. Gunnoe, D.H. Ess, M. Sabat, J. Organomet. Chem. 793 (2015) 248–255.

[17] H.-U. Blaser, H.-P. Buser, R. Häusel, H.-P. Jalett, F. Spindler, J. Organomet. Chem. 621 (2001) 34–38.

[18] a) M.M. Siddiqui, L. Radhakrishna, J.T. Mague, M.S. Balakrishna, J. Organomet. Chem. 824 (2016) 15–24;
b) M.F. Semmelhack, A. Chlenov, D.M. Ho, J. Am. Chem. Soc. 127 (2005) 7759–7773.

[19] a) J. Liu, H. Li, R. Dühren, J. Liu, A. Spannenberg, R. Franke, R. Jackstell, M. Beller, Angew. Chem. Int. Ed. 56 (2017) 11976–11980;
b) K. Dong, R. Sang, X. Fang, R. Franke, A. Spannenberg, H. Neumann, R. Jackstell, M. Beller, Angew. Chem. Int. Ed. 56 (2017) 5267–5271;
c) H. Li, H. Neumann, M. Beller, Chem. Eur. J. 22 (2016) 10050–10056;
d) R. Jennerjahn, I. Piras, R. Jackstell, R. Franke, K.-D. Wiese, M. Beller, Chem. Eur. J. 15 (2009) 6383–6388;
e) C.M. So, Z. Zhou, C.P. Lau, F.Y. Kwong, Angew. Chem. Int. Ed. 47 (2008) 6402–6406;

f) W.C. Fu, Z. Zhou, F.Y. Kwong, Organometallics 35 (2016) 1553–1558;
g) O.Y. Yuen, M. Charoensak, C.M. So, C. Kuhakarn, F.Y. Kwong, Chem. Asian J. 10 (2015) 857–861;
h) J.V. Suárez-Meneses, E. Bonilla-Reyes, E.A. Blé-González, M.C. Ortega-Alfaro, R.A. Toscano, A. Cordero-Vargas, J.G. López-Cortés, Tetrahedron 70 (2014) 1422–1430;
i) A. Zapf, R. Jackstell, F. Rataboul, T. Riermeier, A. Monsees, C. Fuhrmann, N. Shaikh, U. Dingerdissen, M. Beller, Chem. Commun. (2004) 38–39.
[20] D. Pingen, C. Müller, D. Vogt, Angew. Chem. Int. Ed. 49 (2010) 8130–8133.
[21] G.T. Venkanna, H.D. Arman, Z.J. Tonzetich, ASC Catal. 4 (2014) 2941–2950.
[22] X. Liu, H. Nan, W. Sun, Q. Zhang, M. Zhan, L. Zou, Z. Xie, X. Li, C. Lu, Y. Cheng, Dalton Trans. 41 (2012) 10199–10210.
[23] K. Moonen, I. Laureyn, C.V. Stevens, Chem. Rev. 104 (2004) 6177–6216.
[24] C. Anstiss, P. Karuso, M. Richardson, F. Liu, Molecules 18 (2013) 2788.
[25] Catalysts **1a**–**f** bind to solvent molecules that cannot be removed without significant catalyst decomposition. All catalysts demonstrated partial decomposition over long-term high vacuum exposure. The attempts to replace solvent molecules with dichloromethane or deuterated chloroform via co-evaporation by nitrogen flow led to partial decomposition of catalysts as well.
[26] a) M. Shi, M.-J. Qi, X.-G. Liu, Chem. Commun. (2008) 6025–6027;
b) M. Shi, Y.-M. Xu, Angew. Chem. Int. Ed. 41 (2002) 4507–4510.
[27] M. Shi, J.-K. Jiang, Tetrahedron: Asymmetry 13 (2002) 1941–1947.
[28] a) F. Zhong, G.-Y. Chen, Y. Lu, Org. Lett. 13 (2011) 82–85;
b) X.-Y. Guan, Y. Wei, M. Shi, Chem. Eur. J. 16 (2010) 13617–13621.
[29] a) A. Nakano, S. Kawahara, S. Akamatsu, K. Morokuma, M. Nakatani, Y. Iwabuchi, K. Takahashi, J. Ishihara, S. Hatakeyama, Tetrahedron 62 (2006) 381–389;
b) Y. Iwabuchi, M. Nakatani, N. Yokoyama, S. Hatakeyama, J. Am. Chem. Soc. 121 (1999) 10219–10220.
[30] a) M. Shi, Y.-H. Liu, L.-H. Chen, Chirality 19 (2007) 124–128;
b) Y.-H. Liu, L.-H. Chen, M. Shi, Adv. Synth. Catal. 348 (2006) 973–979.
[31] C. Wang, L. Wang, S. Zeng, S. Xu, Z. He, Phosphorus Sulfur Silicon Relat. Elem. 188 (2013) 1548–1554.
[32] N. Utsumi, H. Zhang, F. Tanaka, C.F. Barbas, Angew. Chem. Int. Ed. 46 (2007) 1878–1880.
[33] S.-H. Chen, B.-C. Hong, C.-F. Su, S. Sarshar, Tetrahedron Lett. 46 (2005) 8899–8903.
[34] W.L.F. Armarego, C.L.L. Chai, Purification of Laboratory Chemicals, sixth ed., Butterworth-Heinemann, 2009, 6 ed.
[35] S.T. Handy, J.J. Sabatini, Org. Lett. 8 (2006) 1537–1539.